Energy Spectra Stemming from Interactions of Alfvén Waves and Turbulent Eddies

P. D. Mininni[1,2] and A. Pouquet[2]

[1]*Departamento de Física, Facultad de Ciencias Exactas y Naturales, Universidad de Buenos Aires, Ciudad Universitaria, 1428 Buenos Aires, Argentina*

[2]*NCAR, P.O. Box 3000, Boulder, Colorado 80307-3000, USA*

(Received 24 July 2007; published 21 December 2007)

We present a numerical analysis of an incompressible decaying magnetohydrodynamic turbulence run on a grid of 1536^3 points. The Taylor Reynolds number at the maximum of dissipation is ≈1100, and the initial condition is a superposition of large-scale Arn'old-Beltrami-Childress flows and random noise at small scales, with no uniform magnetic field. The initial kinetic and magnetic energies are equal, with negligible correlation. The resulting energy spectrum is a combination of two components, each moderately resolved. Isotropy obtains in the large scales, with a spectral law compatible with the Iroshnikov-Kraichnan theory stemming from the weakening of nonlinear interactions due to Alfvén waves; scaling of structure functions confirms the non-Kolmogorovian nature of the flow in this range. At small scales, weak turbulence emerges with a $k_\perp^{-2}$ spectrum, the perpendicular direction referring to the local quasiuniform magnetic field.

DOI: 10.1103/PhysRevLett.99.254502 PACS numbers: 47.65.−d, 47.27.Jv, 94.05.Lk, 95.30.Qd

Magnetic fields permeate the Universe, and with the increased resolving capabilities of instruments, a flurry of details on highly complex flows emerge. The origin of such magnetic fields, the dynamo problem, is still not fully understood, in particular, when the magnetic Prandtl number P_M—the ratio of kinematic viscosity ν to magnetic diffusivity η—differs substantially from unity, as it does in the interstellar medium ($P_M \gg 1$) or in convective regions of stars and liquid cores of planets ($P_M \ll 1$). Numerous theoretical and numerical studies have been written (see [1]), and recent laboratory experiments address this fundamental problem as well. Here, we take a different approach by assuming that a dynamo mechanism works, presumably leading to approximate equipartition of the magnetic and kinetic energies, as observed, for example, in the solar wind. We then ask questions about the nature of the nonlinear dynamics of such a flow. The complete problem (a dynamo taken all the way to the nonlinear stage at a high Reynolds number as encountered in nature, and for P_M differing substantially from unity) is still out of reach, but it might be among the key outcomes of petascale computing facilities and experimental devices currently being developed. We specifically address in this Letter the nature of the energy spectra that arise in such conditions. A more detailed account of the development and evolution (up to the peak of enstrophy) of structures and correlations of the flow will be presented elsewhere.

The magnetohydrodynamic (MHD) equations read:

$$\frac{\partial \mathbf{v}}{\partial t} + \mathbf{v}\cdot\nabla\mathbf{v} = -\frac{1}{\rho_0}\nabla\mathcal{P} + \mathbf{j}\times\mathbf{b} + \nu\nabla^2\mathbf{v}, \quad (1)$$

$$\frac{\partial \mathbf{b}}{\partial t} = \nabla\times(\mathbf{v}\times\mathbf{b}) + \eta\nabla^2\mathbf{b}; \quad (2)$$

$\mathbf{v}$ is the velocity, $\mathbf{b}$ is the magnetic field, $\mathbf{j} = \nabla\times\mathbf{b}$ is the current density, $\mathcal{P}$ is the pressure, $\rho_0 = 1$ the density, $\nu = \eta = 2\times10^{-4}$, and $\nabla\cdot\mathbf{v} = \nabla\cdot\mathbf{b} = 0$. One can also write these equations in terms of the Elsässer variables $\mathbf{z}^\pm = \mathbf{v}\pm\mathbf{b}$, of energy $E^\pm$ and flux $\epsilon^\pm$. We solve Eqs. (1) and (2) in a three-dimensional box of length $L_0 = 2\pi$ using periodic boundary conditions and a pseudospectral method, dealiased by the standard 2/3 rule; minimum and maximum wave numbers are $k_{\min} = 1$ and $k_{\max} = N^{1/3}/3$, with $N = 1536^3$ grid points. At all times $k_D/k_{\max} < 1$, where k_D is the dissipation wave number. The initial conditions for the velocity and magnetic fields are constructed from a superposition of three Beltrami (helical) flows to which smaller-scale random fluctuations are added with initial kinetic and magnetic energy $E_V = E_M = 0.5$ [with respective spectra $E_V(k)$ and $E_M(k)$]; magnetic helicity $H_M = \langle\mathbf{a}\cdot\mathbf{b}\rangle \approx 0.45$ ($\mathbf{b} = \nabla\times\mathbf{a}$, where $\mathbf{a}$ is the vector potential, and the brackets denote volume average), and $\cos(\mathbf{v},\mathbf{b}) = \langle\mathbf{v}\cdot\mathbf{b}\rangle\langle|\mathbf{v}||\mathbf{b}|\rangle^{-1} \approx 10^{-4}$ (see [2] for details). The computation is stopped when the growth of the total dissipation saturates ($t = 3.7$), at which time the Reynolds number based on the mechanical integral scale is $R_e = UL_V/\nu \approx 9200$, and that based on the mechanical Taylor scale is $R_\lambda = U\lambda_V/\nu \approx 1100$; U is the rms velocity, the integral scales are defined as $L_i = 2\pi E_i^{-1}\int k^{-1}E_i(k)dk$, the Taylor scales are $\lambda_i = 2\pi[E_i/\int k^2E_i(k)dk]^{1/2}$, and i is either V or M. These scales at $t = 3.7$ are $L_V \approx 2.6$, $\lambda_V \approx 0.31$, $L_M \approx 3.1$, and $\lambda_M \approx 0.39$. It was shown in [2] that at early times, current and vorticity sheets form, and further roll up, fold, or pile up. Here we focus on the fully developed regime close to the peak of enstrophy.

The total energy flux $\Pi(k)$ as a function of wave number at $t = 3.7$ is shown in Fig. 1 (inset), together with the total, kinetic, and magnetic energy spectra [$E(k) = E_V(k) + E_M(k)$], compensated by either $k^{-5/3}$ (Kolmogorov spectrum, hereafter K41) or $k^{-3/2}$ (Iroshnikov-Kraichnan, or IK [3]); the latter takes into account the slowing down of nonlinear transfer because of Alfvén waves. The scaling

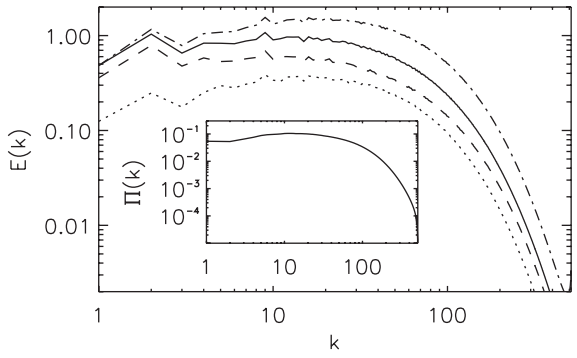

FIG. 1. Energy spectra $E(k)$ (solid line), $E_M(k)$ (dashed line), and $E_V(k)$ (dotted line) compensated by $k^{-3/2}$; $E(k)$ compensated by $k^{-5/3}$ is also shown (dash-dotted line). In the inset is the total energy flux $\Pi(k)$, indicating the extent of the inertial range.

of $E(k)$ and $E_M(k)$ is close to $k^{-3/2}$ in a range of scales covering almost a decade. Energy spectra in MHD have been reported in the literature, both for decaying and forced flows, for data stemming from either numerical simulations or observations (mostly in the solar wind). In most cases, a spectrum close to K41 is found [4], although there are times when the IK solution is preferred [5], and in some cases both scalings may be observed [6]. It is not clear whether universality obtains (in which case, for very large Reynolds numbers it might either be K41 or IK), or whether there are different behaviors, the boundaries to which are not necessarily known. Different spectra have already been observed for different forcings in reduced MHD (RMHD, an approximation valid in the presence of a strong magnetic field) [7], and recently reported for MHD runs with a strong imposed magnetic field [8]. Note that the flow in our run has the largest R_λ obtained in a direct numerical simulation, at the expense, though, of not being stationary.

To clarify the issue of which spectra should arise in MHD turbulence, at least two things can be done. On one hand, one computes isotropic high-order structure functions, in which case the differentiation between K41 and IK is enhanced, as already found in [9]. On the other hand, one can quantify the degree of anisotropy in the flow, something that will be discussed later. We define the longitudinal (parallel to the displacement $\boldsymbol{l}$) structure function of order p for the quantity $\mathbf{f}$ as $S_p^{\mathbf{f}}(\ell) = \langle [\delta f_L(\boldsymbol{l})]^p \rangle = \langle \{[\mathbf{f}(\mathbf{x}) - \mathbf{f}(\mathbf{x}+\boldsymbol{l})] \cdot \boldsymbol{l}/\ell\}^p \rangle$. If the field is self-similar we expect a scaling $S_p^{\mathbf{f}}(\ell) \sim \ell^{\zeta_p^{\mathbf{f}}}$ in the inertial range, where $\zeta_p^{\mathbf{f}}$ are the scaling exponents. In hydrodynamic turbulence, K41 theory predicts $\zeta_p = p/3$, and in MHD the IK theory leads to $\zeta_p = p/4$. In practice, these relations are modified by intermittency corrections due to extreme events at the small scales. The exact scaling laws for MHD turbulence derived in [10], $\langle \delta z_L^{\mp}(\boldsymbol{l}) |\delta \mathbf{z}^{\pm}(\boldsymbol{l})|^2 \rangle = -4\epsilon^{\pm}\ell/3$, can be used to define the inertial range and to improve the estimate of the scaling exponents, as is often done in hydrodynamics when the extended self-similarity (ESS) hypothesis is used [11]. These scaling laws, and structure functions up to order 8, were computed at $t = 3.7$ for increments in the $\hat{x}$, $\hat{y}$, and $\hat{z}$ directions, and averaged. Figure 2 shows the resulting scaling exponents $\zeta_p^{\pm}$ for the Elsässer fields $\mathbf{z}^{\pm}$, computed in the range in which the exact scaling laws hold.

Consistent with the computation of the energy spectra, the scaling of $\mathbf{z}^{\pm}$ is closer to the IK prediction, with $\zeta_3^{+} = 0.831 \pm 0.006$, $\zeta_3^{-} = 0.806 \pm 0.005$, $\zeta_4^{+} = 0.985 \pm 0.008$, and $\zeta_4^{-} = 0.958 \pm 0.007$ (for higher orders, deviations from K41 and IK are larger because of intermittency corrections). The values of $\zeta_3^{\pm}$ are not consistent with the exact scaling law for hydrodynamic turbulence. As stated in [10], the exact scaling laws in MHD involve correlations between the velocity and magnetic fields (or equivalently between $\mathbf{z}^{\pm}$), and such correlations play a role in the dynamics of the flow. In particular, they can induce a shift from a standard K41 coupling; this effect has been modeled in [12] as a scale variation of the angle between the velocity and magnetic field, i.e., in the relative cross helicity $\cos(\mathbf{v}, \mathbf{b})$. Also, from the values of $\zeta_3^{\pm}$ and $\zeta_4^{\pm}$, the possibility of a Kolmogorov scaling hidden by a bottleneck (as reported in [13]) can be ruled out for this simulation. However, even when the scaling exponents in the inertial range for $p = 3$ and 4 are closer to the IK prediction (with strong corrections due to intermittency), it is worth mentioning that the structure functions after using ESS do not show the same scaling at all scales. This is different from the hydrodynamic case where, after using the ESS hypothesis, a unique scaling at all scales is observed, even in the dissipative range. This brings us to our second point, linked to anisotropy.

Indeed, it is known that in MHD anisotropy develops at small scales under the influence of a large-scale magnetic field. Several models have been written to explain how this

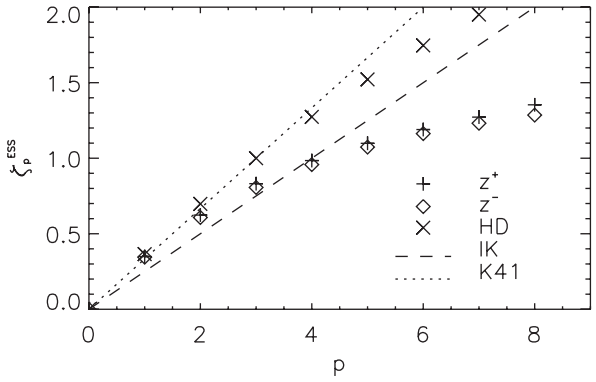

FIG. 2. Scaling exponents $\zeta_p^{\pm}$ for $\mathbf{z}^{\pm} = \mathbf{v} \pm \mathbf{b}$. The K41 (dotted line) and IK (dashed line) predictions are indicated. As a reference, the scaling exponents in a 1024^3 hydrodynamic (HD) simulation are also shown [21]. Note $\zeta_4^{\pm} \sim 1$, while for HD $\zeta_3 \sim 1$.

might affect the small-scale dynamics. The weak turbulence (WT) theory [14] leads to an exact spectrum $\sim k_\perp^{-2} f(k_\parallel)$, where $k_\parallel$ and $k_\perp$ are the amplitudes of the wave vectors in the directions parallel and perpendicular to a uniform magnetic field $\mathbf{B}_0$. It has long been argued that at high Reynolds number, leading to a large-scale separation, the large-scale magnetic field $\mathbf{B}_{\rm LS}$ plays the same dynamical role as $\mathbf{B}_0$. As a result, we can expect the small scales to be anisotropic with respect to $\mathbf{B}_{\rm LS}$. However, since $\mathbf{B}_{\rm LS}$ evolves in time with a characteristic correlation time $\tau_{\rm LS}$ and has a curvature proportional to the Taylor scale λ_M, in the absence of $\mathbf{B}_0$ and for isotropic initial conditions, one may assume that isotropy is still preserved in the large and intermediate scales ($\ell \gtrsim \lambda_M$).

To illustrate this, we follow the procedure given in [15]. A local mean field $\mathbf{B}_{\rm LS}(\mathbf{x})$ is computed as the average of the magnetic field $\mathbf{b}$ in a box of size L_M with center on $\mathbf{x}$, such as $\mathbf{B}_{\rm LS} = \langle \mathbf{b} \rangle_{{\rm box}(L_M,\mathbf{x})}$. Then, unit vectors $\boldsymbol{l}_\parallel$ and $\boldsymbol{l}_\perp$ ($\parallel$ and $\perp$ with respect to $\mathbf{B}_{\rm LS}$) are defined, and the two following longitudinal magnetic structure functions

$$S^{\mathbf{b}}_{2\perp}(\ell) = S^{\mathbf{b}}_2(\ell \boldsymbol{l}_\perp), \qquad S^{\mathbf{b}}_{2\parallel}(\ell) = S^{\mathbf{b}}_2(\ell \boldsymbol{l}_\parallel), \tag{3}$$

are computed for all points in the vicinity of $\mathbf{x}$ and for $\ell \in [2\pi k_{\rm max}^{-1}, L_M/2]$. The process is repeated for several values of $\mathbf{x}$, and $S^{\mathbf{b}}_{2\perp}$ and $S^{\mathbf{b}}_{2\parallel}$ are averaged over all the boxes (the results shown are the average over $\approx 10^7$ points). Figure 3 gives the resulting $S^{\mathbf{b}}_{2\perp}$ and $S^{\mathbf{b}}_{2\parallel}$, as well as their ratio. In the limit $\ell \to 0$, this ratio can be associated with one of the so-called Shebalin angles [16]

$$\tan^2(\theta) = 2 \lim_{\ell \to 0} \frac{S^{\mathbf{b}}_{2\perp}(\ell)}{S^{\mathbf{b}}_{2\parallel}(\ell)}, \tag{4}$$

which measures the anisotropy of $\mathbf{b}$ with respect to $\mathbf{B}_{\rm LS}$.

We see that scales smaller than $\ell \approx 0.4$ are anisotropic, in agreement with [15]; $S^{\mathbf{b}}_{2\perp}(\ell) > S^{\mathbf{b}}_{2\parallel}(\ell)$ in this range. However, isotropy obtains in an intermediate range of scales corresponding roughly to the $-3/2$ range in Fig. 1. For very small increments ($\ell \leq 0.02 \approx 2\pi k_D^{-1}$), both structure functions follow $\sim \ell^2$ scaling, as expected for smooth fields in the dissipative range. At scales larger than the dissipation scale, but smaller than $\ell \approx 0.4 \approx \lambda_M$, a range with $S^{\mathbf{b}}_{2\perp} \sim \ell$ is observed, consistent with a $k_\perp^{-2}$ scaling in the spectrum as predicted by WT theory [14]. In the range $\ell \approx [0.4, 1.2]$, where fluctuations are roughly isotropic, $S^{\mathbf{b}}_{2\perp} \sim S^{\mathbf{b}}_{2\parallel} \sim \ell^{1/2}$. Figure 4 shows the structure functions compensated by $\ell^{1/2}$ (IK scaling) and $\ell^{2/3}$ (K41). The $\sim \ell^{1/2}$ scaling is again consistent with the isotropic energy spectrum and scaling of the isotropic ($p = 3$ and 4) structure functions discussed previously.

The recovery of isotropy observed at intermediate scales should not be associated with the small-scale fluctuations but rather with the fluctuations of the large-scale magnetic field, and thus may not always take place. Note that $\tan^2(\theta) > 1$, and for very small ℓ, we have $S^{\mathbf{b}}_{2\perp} \sim S^{\mathbf{b}}_{2\parallel} \sim \ell^2$. If $\mathbf{B}_{\rm LS}$ is strong, and there is enough scale separation for the local mean field to look as a uniform field for the small scales, WT theory is consistent with $S_{2\parallel}(\ell) \sim \ell^{1/2}$. For $S_{2\perp}(\ell) \sim \ell^\alpha$ with $\alpha \geq 1/2$, the structure functions satisfy $S_{2\perp}/S_{2\parallel} \geq 1$ at all scales.

Let λ_M be the largest scale for the fluctuations to see the mean magnetic field as a uniform field; for $\ell \approx \lambda_M$, the curvature of the large-scale magnetic field cannot be neglected, and fluctuations become more isotropic. At scales larger than λ_M, we thus have isotropic fluctuations with a local mean magnetic field $\mathbf{B}_{\rm LS}$. Assuming for simplicity equipartition (see, e.g., [17] for extensions of the phenomenology to the nonequipartition case), and constant energy flux $\varepsilon \sim u_\ell^2 \tau_{{\rm A},\ell}/\tau_{{\rm NL},\ell}^2$ [where $\tau_{{\rm NL},\ell} \sim \ell/v_\ell$ is the nonlinear turnover time, and $\tau_{{\rm A},\ell} \sim \ell/B_{\rm LS}$ is the Alfvén crossing time (see [18] for a review of the relevant time scales in MHD)], we obtain $b_\ell \sim v_\ell \sim \ell^{1/2}$ and the IK energy spectrum $E(k) \sim k^{-3/2}$. At scales smaller than λ_M, the fluctuations are anisotropic and several phenomenologies have been put forward [12,14,19]. Assuming v_l and b_l are mostly in the direction perpendicular to $\mathbf{B}_{\rm LS}$, $\tau_{{\rm NL},l} \sim \ell_\perp/v_l$. The anisotropic extension of IK takes the Alfvén time as $\tau_{{\rm A},l} \sim \ell_\parallel/B_{\rm LS}$, which results in $v_l \sim b_l \sim \ell_\perp \ell_\parallel^{-1/2}$

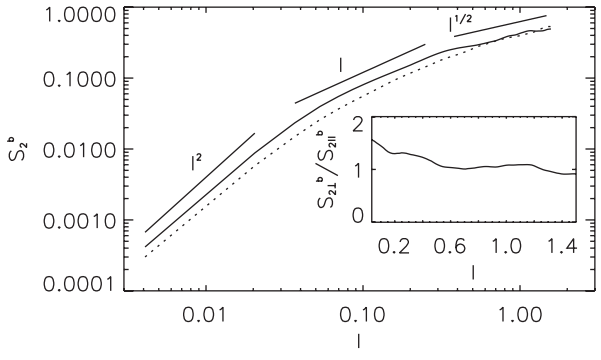

FIG. 3. Second order structure functions $S^{\mathbf{b}}_{2\perp}(\ell)$ (solid line) and $S^{\mathbf{b}}_{2\parallel}(\ell)$ (dotted line). Several slopes are given as a reference. The inset shows the ratio $S^{\mathbf{b}}_{2\perp}(\ell)/S^{\mathbf{b}}_{2\parallel}(\ell)$ in linear coordinates.

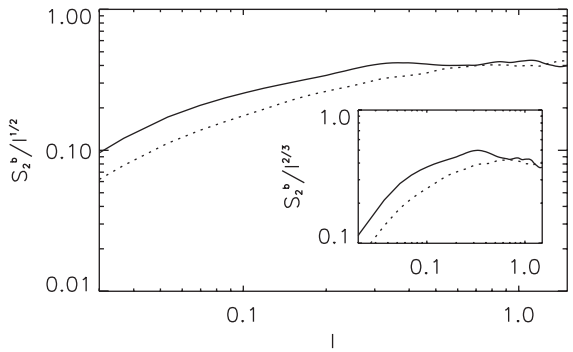

FIG. 4. $S^{\mathbf{b}}_{2\perp}$ (solid line) and $S^{\mathbf{b}}_{2\parallel}$ (dotted line) compensated by $\ell^{1/2}$. The inset shows the same quantities compensated by $\ell^{2/3}$.

and the spectrum $E(k) \sim k_\perp^{-2} k_\parallel^{1/2}$. In the context of this run, where the correlation length of the large-scale magnetic field is L_M, we can assume $\tau_{A,l} \sim L_M/B_{LS}$, which leads to the same $\sim \ell_\perp$ and $\sim k_\perp^{-2}$ scaling. Note that this $\perp$ spectrum is what WT theory predicts, and that for the isotropic case ($k_\perp \sim k_\parallel$), $E(k) \sim k_\perp^{-2} k_\parallel^{1/2}$ turns into the IK spectrum. In this light, it is not surprising that the IK spectrum at large scales can be followed, in the same dynamical vein, by its wave turbulence anisotropic counterpart at small scales.

A different MHD spectrum has been advocated in [19], whereby the anisotropy of the flow induces a Kolmogorov spectrum. In the anisotropic range, this implies $S^{\mathbf{b}}_{2\perp} \sim \ell^{2/3}$. Another anisotropic model based on dynamic alignment of the velocity and magnetic fields [12] implies $S^{\mathbf{b}}_{2\perp} \sim \ell^{1/2}$. Such scalings are not observed in our computation, and the results in Fig. 4 suggest $S^{\mathbf{b}}_{2\perp} \sim \ell$ is a better fit in the anisotropic range of our run.

In conclusion, we presented evidence of energy scaling compatible with IK phenomenology in data stemming from a high resolution simulation of a freely decaying MHD flow. This scaling is observed at intermediate scales where the turbulent fluctuations are approximately isotropic. By decomposing the fields into their components parallel and perpendicular to the local mean magnetic field, we confirmed the scaling and showed the emergence of a $k_\perp^{-2}$ spectrum at smaller scales. This is consistent with anisotropic extensions of the IK spectrum and with predictions from weak turbulence theory. The behavior differs from scaling laws observed in previous numerical simulations or predicted by some theories of MHD turbulence. However, other scaling laws cannot be ruled out completely for the following reasons. The various scaling exponents discussed result from the relevant time scales associated with the energy transfer [18]. MHD turbulence transfer is nonlocal [20], with time scales associated with the large and the small scales, and a breakdown of universality can be a candidate to explain the variety of solutions reported in the literature. As an example, it is useful to compare the present results with simulations of forced MHD turbulence. In our simulations we can associate the scale where the transition from the isotropic to anisotropic field takes place with λ_M, and the correlation time of the local mean field τ_{LS} with L_M/B_{LS}. In a forced simulation, the correlation time of the large-scale magnetic field is proportional to the correlation of the external forcing τ_F. If $\tau_F \ll \tau_{A,\ell}$, the local mean field changes faster than the Alfvén wave crossing time at ℓ, and we should not expect anisotropy to develop or wave interactions to be relevant. The scale where the transition takes place would change accordingly. Such a dependence would be consistent with results from forced RMHD [7] and MHD simulations [8].

We acknowledge discussions with D. C. Montgomery; P. D. M. acknowledges discussions with D. O. Gómez. The NSF-CMG Grant No. 0327888 was instrumental in our work. Computer time was provided by the NCAR BTS program. P. D. M. is a member of the Carrera del Investigador Científico of CONICET.

[1] A. Brandenburg and K. Subramanian, Phys. Rep. **417**, 1 (2005).
[2] P. D. Mininni, A. G. Pouquet, and D. C. Montgomery, Phys. Rev. Lett. **97**, 244503 (2006).
[3] P. S. Iroshnikov, Sov. Astron. **7**, 566 (1963); R. H. Kraichnan, Phys. Fluids **8**, 1385 (1965).
[4] M. K. Verma, D. A. Roberts, and M. L. Goldstein, J. Geophys. Res. **100**, 19839 (1995); M. K. Verma *et al.*, J. Geophys. Res. **101**, 21619 (1996); D. Biskamp and W.-C. Müller, Phys. Plasmas **7**, 4889 (2000).
[5] W.-C. Müller and R. Grappin, Phys. Rev. Lett. **95**, 114502 (2005).
[6] J. J. Podesta, D. A. Roberts, and M. L. Goldstein, Astrophys. J. **664**, 543 (2007).
[7] P. Dmitruk, D. O. Gómez, and W. H. Matthaeus, Phys. Plasmas **10**, 3584 (2003).
[8] J. Mason, F. Cattaneo, and S. Boldyrev, arXiv:0706.2003.
[9] H. Politano, A. Pouquet, and V. Carbone, Europhys. Lett. **43**, 516 (1998); D. Biskamp and W.-C. Müller, Phys. Plasmas **7**, 4889 (2000).
[10] H. Politano and A. Pouquet, Phys. Rev. E **57**, R21 (1998); Geophys. Res. Lett. **25**, 273 (1998).
[11] R. Benzi *et al.*, Europhys. Lett. **24**, 275 (1993); Phys. Rev. E **48**, R29 (1993).
[12] S. Boldyrev, Phys. Rev. Lett. **96**, 115002 (2006).
[13] N. E. L. Haugen, A. Brandenburg, and W. Dobler, Phys. Rev. E **70**, 016308 (2004).
[14] S. Galtier, S. V. Nazarenko, A. C. Newell, and A. Pouquet, J. Plasma Phys. **63**, 447 (2000).
[15] L. J. Milano, W. H. Matthaeus, P. Dmitruk, and D. C. Montgomery, Phys. Plasmas **8**, 2673 (2001).
[16] J. V. Shebalin, W. H. Matthaeus, and D. Montgomery, J. Plasma Phys. **29**, 525 (1983).
[17] Zhou and W. H. Matthaeus, Phys. Plasmas **12**, 056503 (2005).
[18] A. Pouquet, U. Frisch, and J. Leorat, J. Fluid Mech. **77**, 321 (1976); Y. Zhou, W. H. Matthaeus, and P. Dmitruk, Rev. Mod. Phys. **76**, 1015 (2004).
[19] P. Goldreich and S. Sridhar, Astrophys. J. **438**, 763 (1995).
[20] A. Alexakis, P. D. Mininni, and A. Pouquet, Phys. Rev. E **72**, 046301 (2005); P. D. Mininni, A. Alexakis, and A. Pouquet, Phys. Rev. E **72**, 046302 (2005).
[21] A. Alexakis, P. D. Mininni, and A. Pouquet, Phys. Rev. Lett. **95**, 264503 (2005).